

MATRIX-FRACTURE INTERACTION IN SINGLE MATRIX BLOCKS

E. R. Rangel-German and A. R. Kavscek

Stanford University
Green Earth Sciences, Room 067
Stanford, CA, 94305, USA
e-mail: edgarr@pangea.stanford.edu
kavscek@pangea.stanford.edu

ABSTRACT

Capillary imbibition is an important mechanism during water reinjection in fractured porous media. Using an X-ray computerized tomography (CT) scanner, and a novel, CT-compatible core holder, we performed a number of experiments to study air expulsion from rock samples by capillary imbibition of water in a three-dimensional geometry. Different injection rates and fracture apertures were utilized.

The existence of two flow periods during imbibition by the matrix was observed. The early-time period can be understood as an infinite acting media and the square root of time model of imbibition with the appropriate characteristic time and length can be used. Although the late-time period has not been analyzed fully, a set of both characteristic times and lengths is proposed.

Two different fracture flow regimes were also identified. The first one, named "filling-fracture" shows a variable length plane source due to relatively slow water flow through fractures; the second flow regime, named "instantly-filled fracture", where the time to fill the fracture is much less than the imbibition time, shows a constant plane source imbibition. The behavior of the second regime is very similar to that observed in both counter current and cocurrent one-dimensional imbibition experiments reported previously in the literature.

INTRODUCTION

In common geothermal reservoirs, the rate of mass transfer between the rock matrix and fractures usually determines the amount of water in the matrix.

Intuitively, injected water will prefer to flow through the fractures rather than the low-permeability matrix

in naturally fractured reservoirs when capillary imbibition forces are weak. Unless imbibition forces are strong enough to pull water into the matrix, there will be no mass transfer between matrix and fractures. Imbibition forces must be strong enough for water injection to be successful. If not, water will propagate through the fracture network with little imbibition into the matrix and the injection will fail. (Akin, et. al, 1999.) Capillary forces in reservoir rocks depend on factors such as permeability, pore structure, pore-throat to pore-body size ratio, wettability, and the interfacial tension between the resident and the imbibing phase.

When speaking of fractured media, one has to consider the properties that make this system different from the homogeneous case. Several studies have focused on understanding the properties of fractured porous media such as capillary pressure, continuity between adjacent matrix blocks, fracture relative permeabilities, cocurrent or counter-current imbibition (Kazemi et al. 1989; Mattax and Kyte 1962; Hughes 1995, Cil et al. 1998; Rangel-German et al. 1998).

Capillary imbibition is an important mechanism in fractured porous media. Previous experimental work regarding imbibition has examined the scaling aspects of the process in order to estimate oil recovery from reservoir matrix blocks that have shapes and sizes different for those of laboratory core samples (Handy 1960; Morrow 1994; Ma 1995; Cil and Reis 1996; Garg et al. 1996; Zhang et al. 1996; Akin et al. 1999; Reis and Cil 1999(a, b)).

Handy (1960) in describing air/water systems stated that imbibition could be described by either a diffusion-like equation or a frontal-advance equation, depending on assumptions. However, both solutions predict that the mass of water imbibed depends linearly on the square root of time in one-dimensional media. This has been verified by other studies (Reis

and Cil 1993; Cil and Reis 1996; Reis and Haq 1999). In the case of oil, a number of experimental data for oil recovery in fractured media have been reported in the literature (Kazemi et al. 1989; Mattax and Kyte 1962.)

Reis and Cil (1999) concluded that the best models for the early-time period, are the square root and linear-saturation-profile models. They proposed an empirical power-law-based model for the late-time period. This last model cannot be extrapolated to early-time periods.

Other studies have applied rigorous mathematical analysis to model pore-scale imbibition to find ultimately matrix-fracture transfer functions for naturally fractured reservoirs (Mogensen and Stenby 1998; Reis and Cil, 1999; Reis and Haq 1999).

In this paper, we describe the preliminary results of an experimental study of air expulsion from rock samples by capillary imbibition of water in a three-dimensional geometry. A laboratory flow apparatus was built to obtain data on water-air displacements in horizontal single-fracture systems. Flow in the matrix and fracture is imaged simultaneously. During the experiments, porosity and saturation calculations along the cores were made utilizing an X-ray computerized tomography (CT) Scanner.

This paper also describes an approximate approach to calculate the amount of water imbibing into a rock based on hydraulic diffusivity. Thus, characteristic times are distinguished. An easy way to obtain iso-saturation curves is explained too. Matching the experimental data validated this method.

EXPERIMENTAL DESIGN AND PROCEDURE

A novel experimental set-up was designed to insure minimal artifacts while scanning and the collection of maximum saturation information. First, the coreholder is described and then the CT scanner and experimental procedure.

Coreholder. Due to the cubic shape of the cores and the desire to measure in-situ saturations through the use of the CT Scanner, conventional core holders could not be used. A novel, CT-compatible imbibition coreholder was designed. The basic idea behind it is to avoid drastic changes of density of the object scanned and present circular cross-sections to the scanner. We initially coated and sealed the samples with Marine Epoxy (Tap Marine Plastic #314). The cores were then potted in vertical

cylindrical PVC containers with the same epoxy. We used a cylindrical shape to allow the core to be rotated in any position desired around the vertical axis.

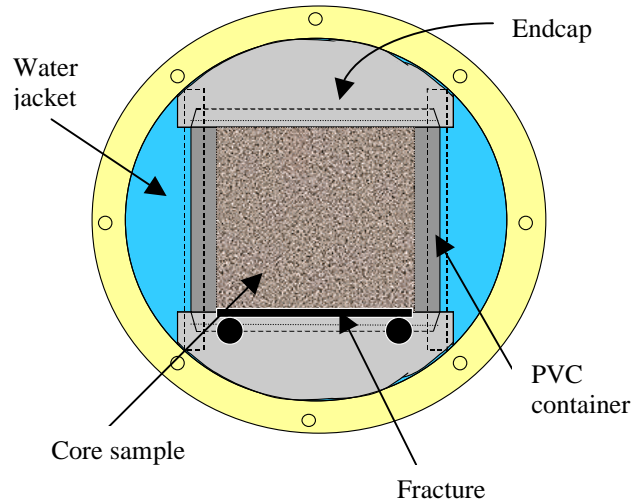


Figure. 1. The Core Holder. Frontal View.

Once the core was epoxied in the PVC container, the bottom face of the cylinder was cut open so one face of the original cube could be exposed to the water flow.

This PVC holder was then placed in a second horizontal cylindrical acrylic container as shown in Fig.1. Again we used a cylindrical shape to allow the core to now be rotated in any position around the horizontal axis. Once filled with water, the second container works as a water jacket to lessen the contrast in density between the acrylic and PVC/Epoxy. Thus, the cross-sectional shape for scanning is symmetric and circular.

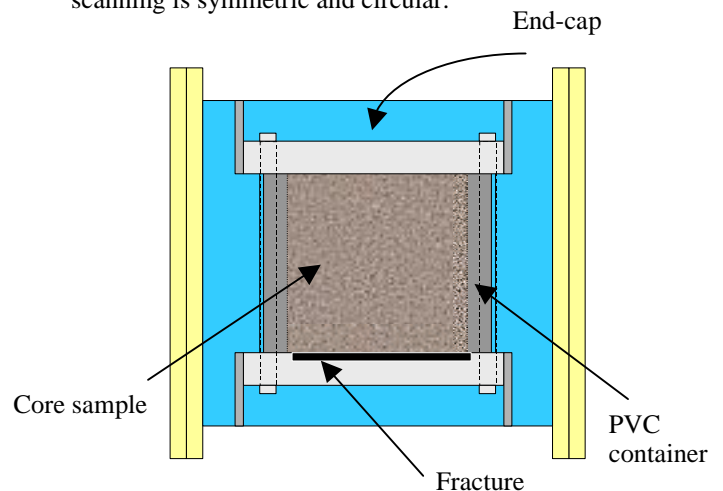


Figure. 2. The Core Holder. Lateral View.

Acrylic end-caps were machined to mate with the circular PVC coreholder and at the same time to have 2 perforations to emulate horizontal 'wells' along the corners of the core. The end-caps (one at the top and one at the bottom) were attached to the PVC coreholder by means of screws and sealing O-rings. With this system one can inject and produce fluids in any combination desired within the four ports. The end-caps are also shaped so that core and end-caps fit the inner diameter of the water jacket when assembled. The acrylic end-caps and core are shown in Figs. 1, 2 and 3. This combination of end-caps allowed us to set the coreholder in a unique position, which is crucial to guarantee accurate porosity and saturation calculations with the CT scanner. Calculations based on CT numbers basically consist of subtractions of CT images at the same position, hence the importance of enabling the coreholder to be re-placed at the desired position.

Fracture apertures were set by means of metallic shims (essentially feeler gauges of precise thickness) placed on the sides orthogonal to the 'wells'. Thus we guaranteed an even fracture aperture along the entire core.

In summary, Figures 1 to 3 show a diagram of the coreholder used in this work. We found that this set-up reduces X-ray artifacts, improving the resolution of the CT images.

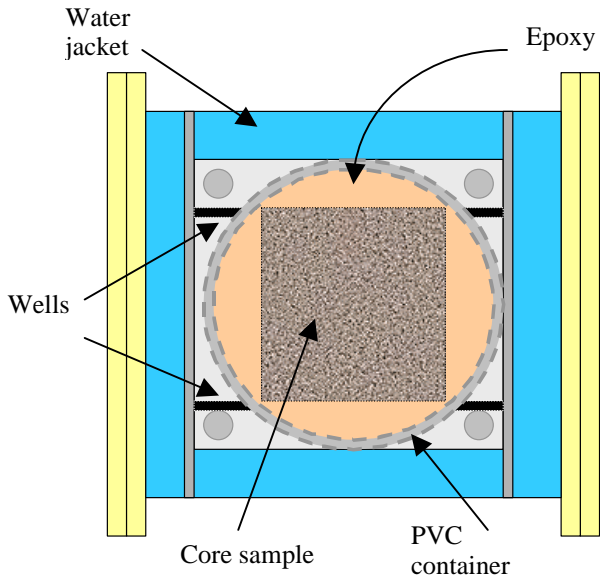


Figure. 3. The Core Holder. Top View.

CT Scanner. A CT Scanner can be used to measure porosity, saturation and in some cases, concentration distribution, and to track advancing fronts. It can also be used to measure fracture apertures. We used a modified Picker 1200SX Dual Energy CT scanner.

Procedure. Rather than scan in a conventional mode where the X-ray CT data is collected in cylindrical volume sections that are normal to the central horizontal axis of the core, the entire height of the core is scanned in a single shot. That is, Fig. 1 represents the cross-section imaged. Because we scan along the direction of imbibition (either vertical or horizontal), a single slice provides us with an image of the progress and saturation pattern of imbibition as well as the progress of the water flow in the fracture.

Different experiments at constant water injection rates into the fracture were performed. Using a Constametric pump, rates varied from very slow to very high. We also used different fracture apertures, going from very narrow (0.0025mm) to wide (0.1 mm). Setting the flow rate and having fixed the fracture thickness, we obtained CT images to observe the progress of imbibition.

For the experiments reported here, we injected water on the left 'horizontal well' and produced from the right hand side. The idea was to have uniform flow along the bottom face of the core; i.e. water flow through the fracture. Once the injection started we scanned at different times at the same location.

The water and air saturations were calculated from the CT images. The following equation shows how to evaluate water saturation for the water displacing air case:

$$S_w = \frac{CT_{aw} - CT_{cd}}{CT_{cw} - CT_{cd}} \dots\dots\dots (1)$$

where CT_{aw} is the CT number for water and air saturated core at a matrix location, CT_{cd} is the CT number for the dry core at a matrix location, and CT_{cw} is the CT number for a 100% water saturated core.

Cores. For this work, we used cubic Berea sandstone rock samples. All were 5 x 5 x 5 cm blocks. Using the CT numbers obtained from the experiments, porosity along the cores was determined. The most common way to calculate porosity from CT images is by using the following expression (Withjack, 1988):

$$\phi = \frac{CT_{cw} - CT_{cd}}{CT_w - CT_a} \dots\dots\dots (2)$$

where CT_w is the CT number for water, and CT_a is the CT number for air. The CT number for water is around 0 (zero), while the CT number for air is minus 1000. Figure 4 shows the porosity distribution of one volume section of the rock. The average porosity is 25% and the distribution is relatively narrow (standard deviation = 2%) indicating homogeneity.

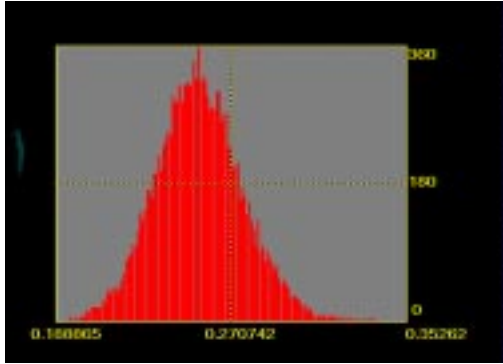


Figure. 4. Porosity Distribution of Berea Sandstone sample.

EXPERIMENTAL RESULTS

Following the aforementioned procedure, images such as that shown in Fig. 5 were collected throughout the experiment. Figure 5 corresponds to 10 min (0.32 PV) of water injection.

An important characteristic that we observed during these experiments was the presence of two different fracture-flow regimes.



Figure. 5. CT Saturation Image for 0.32 PV injected. "Filling-fracture." Aperture = 0.1 mm.

The first one, named "filling-fracture" shows a variable plane source due to relatively slow water flow through fractures. Even though production is seen early in this regime, we believe the fracture is never completely filled and the water horizontal advance is controlled by the interaction between the matrix and the fracture. An example of this kind of regime can be seen in Figure 5. We expect that the advance of water in the horizontal and vertical directions each scales linearly with square root of time. Thus, we anticipate that the mass of water imbibed scales linearly with time because it is proportional to the product of these two length scales.

The second regime, named "instantly-filled fracture", where the time to fill the fracture is much less than the imbibition time, shows a constant plane source imbibition. We found that the behavior of the second regime is very similar to that observed in both counter current and cocurrent imbibition experiments reported previously in the literature. An example of this kind of regime can be seen in Figure 6. The image in Fig. 6 is very nearly one-dimensional advance and so we expect the mass of water to scale linearly with the square root of time.



Figure. 6. CT Saturation Image for 0.32 PV injected. "Instantly-Filled fracture." Aperture = 0.0025 mm.

Calculating the average water saturation (S_w) of the block at each time, and plotting S_w against the square root of time or against time, one obtains the curves shown in Figure 7 and Figure 8, respectively. The average water saturation is, of course, proportional to the mass of water imbibed. In Figure 7, it can be seen that the "instantly-filled fracture" system fits a straight-line trend; whereas on Figure 8, one can see that the "filling fracture" system fits the straight-line trend. Both figures show two different periods. Firstly, there is a linear behavior where the porous medium behaves like an infinite one, the water imbibes without being affected by the boundaries of the rock.

From these observations we establish that early-time behavior can be approximated by means of the square root of time model for the “instantly-filled fracture” system as long as we used the appropriate characteristic times and lengths. Secondly, once the boundaries make their presence felt on imbibition, there is a late-time and non-linear behavior.

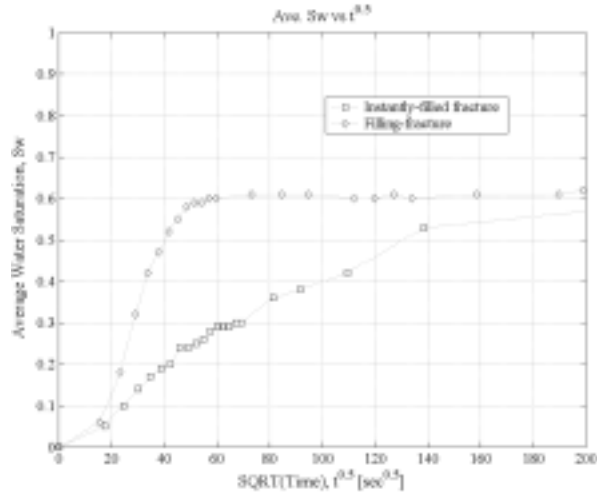


Figure. 7. Average saturation versus square root of time.

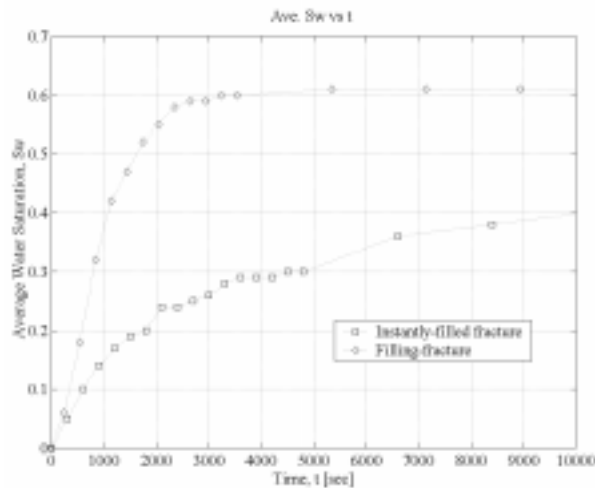


Figure. 8. Average saturation versus time.

SEMI-ANALYTICAL IMBIBITION MODEL

As mentioned earlier, this paper focuses mainly on the solution for early-time behavior of imbibition.

Filling-fracture regime. This regime is caused by relatively slow water flow through fractures. A set of images like that shown in Figure 5 obtained for different times and allowing us to analyze the progress of imbibition is shown in Figure 9. Setting the image color bar to display the maximum water saturation observed in the experiments ($S_w = 0.62$), we obtain a set of images where the shape and position of the front of the iso-saturation curve for 62% is tracked.

The first step is to obtain expressions for the horizontal and vertical advance as a function of time, i.e. functions $x_D = x_D(t^{1/2})$ and $y_D = y_D(t^{1/2})$. These functions were obtained from the experimental results. Figure 10 shows the curves obtained and used for the calculations in this paper. Equations 3 and 4 show their analytical expressions.

$$x_D = 0.0482\sqrt{t} - 0.3219 \dots\dots\dots (3)$$

and

$$y_D = 0.0282\sqrt{t} - 0.1686 \dots\dots\dots (4)$$

We tried to describe the imbibition process by a diffusion-like equation with the frontal-advance experimentally analyzed. We applied a linear superposition of 1-D solutions of the diffusion equation (Carslaw and Jaeger, 1959):

$$S_w(Y, t) = \text{erfc}\left(\frac{Y}{2\sqrt{\alpha t}}\right) \dots\dots\dots (5)$$

where Sw is the water saturation, Y is the vertical position of the iso-saturation S_w in meters; t is the time in seconds, and α is the hydraulic diffusivity in m^2/sec .

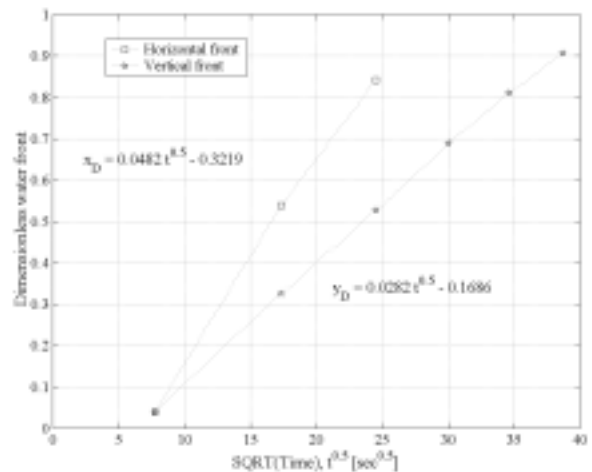


Figure. 10. Horizontal and Vertical water front advance versus square root of time.

Based on the experimental data and using Equation 4, we can calculate the time for any desired dimensionless vertical position $y_D = y/H$ (y = vertical position in m, and H the entire height of the core, in m). Then by means of Equation 5 and an optimization technique, we estimated the value of the hydraulic diffusivity, α ($\alpha = 0.001 \text{ cm}^2/\text{s}$).

We calculated the horizontal position of the front by means of Equation 3; then, using Equation 5, with the estimated value for hydraulic diffusivity, we can calculate the vertical position of the iso-saturation, S_w , we desire. The resulting plot can be seen in Figure 11.

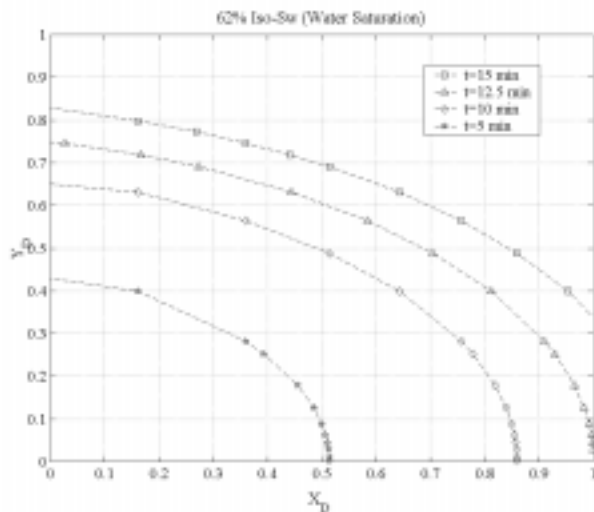


Figure. 11. Water Iso-Saturation curves for different times obtained with new approach.

Instantly-filled fracture regime. This regime is very similar to that observed in both counter current and cocurrent one-dimensional imbibition experiments previously reported in the literature. Our experimental results for the instantly-filled fracture regime showed that a linear relation can be found if S_w data is plotted against $t_D^{1/2}$. The analytical expression for this relation was first presented by Handy (1960):

$$m = \rho_w A \left(\frac{2P_c k \phi S_w}{\mu_w} \right)^{1/2} t^{1/2} \dots\dots\dots (6)$$

where m is the mass of water imbibed, ρ_w is the density of water, A is the cross-sectional area, P_c is

the capillary pressure, k is the permeability to water, ϕ is the porosity, S_w is the wetting phase saturation, μ_w is the wetting-phase viscosity, and t is the time.

The linear relation between the mass imbibed and the square root of time is apparent and the slope is proportional to the square root of imbibition potential, $P_c k S_w$. (Akin et al., 1999).

CHARACTERISTIC TIMES AND LENGTHS FOR SCALING

Laboratory experiments are an easy way to study the processes that occur in real geothermal reservoirs. However every datum obtained from them must be scaled to reservoir conditions to be meaningful. Lab values may come from experiments on matrix blocks with shapes, sizes and boundary conditions very different from those of the real conditions. In this paper, we propose a set of both characteristic times and lengths that can help us to scale these parameters and further obtain a model for imbibition for late-time period behavior.

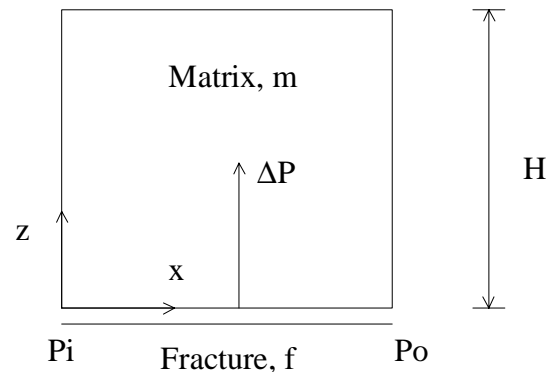


Figure. 12. Diagram of the experiment for mathematical analysis.

Writing the flow equations for the experiment with the parameters and geometry shown in Figure 12, and using the one assumption of zero gradient of non-wetting phase pressure with respect to the height ($dP_{nw}/dz = 0$.) we found the scaling parameters as described below. Different sets were obtained for matrix and fracture systems.

Fracture System. For this system we do not require any assumption. We found:

$$x_D = \frac{x}{L} \dots\dots\dots (7)$$

$$p_D = \frac{p}{p_o} \dots\dots\dots (8)$$

$$t_D = \frac{t}{t_f^*} \dots\dots\dots (9)$$

where t_f^* is the characteristic time for the fracture defined as:

$$t_f^* = \frac{L^2 \mu_w \phi}{p_o k} \dots\dots\dots (10)$$

From this characteristic time we established that the fracture fills instantly with respect to the matrix if $t_D \gg 1$.

Matrix System. This system is more complicated than the fracture but with the zero non-wetting phase pressure gradient we found:

$$z_D = \frac{z}{H} \dots\dots\dots (11)$$

$$p_D = \frac{p \left(\frac{k}{\phi} \right)^{1/2}}{\sigma} \dots\dots\dots (12)$$

where σ is the interfacial tension.

$$t_D = \frac{t}{t_m^*} \dots\dots\dots (13)$$

where t_m^* is the characteristic time for the matrix defined as:

$$t_m^* = \frac{H^2 \mu_w}{\sigma \left(\frac{k}{\phi} \right)^{1/2}} \dots\dots\dots (10)$$

SUMMARY AND CONCLUSIONS

The apparatus described here was used to obtain detailed measurements of flow rates, porosity, and saturation distribution, and to study the progress and saturation pattern of imbibition as well as the progress of the water flow in the fracture. CT imaging of the imbibition process permits observation of the advance of the water front into the

cores and explains the observed trends in water saturation as a function of time.

Phase distribution in the matrix and inside the fracture was determined by means of a (CT) Scanner. The novel coreholder permits imaging of the entire length of the matrix block with a single shot improving the quality of the CT images. Several tests were performed on Berea sandstone sample machined from a block of outcrop material. These tests confirmed the repeatability of the method.

This work strengthens the idea that both capillary and viscous forces dominate the interaction between matrix and fracture. We found that the square-root of time model matches very accurately the experimental data for the early-time period. Moreover, a semi-analytical approach for determining the saturation distribution based on hydraulic diffusivity was presented. This approach can be used to obtain a matrix-fracture transfer function. This model seems to fit the experimental data with reasonable accuracy.

More experimental data and further analysis are needed in order to find a relation to couple the hydraulic diffusivity term, α , with the fracture thickness for a more general model that covers any fracture aperture. We believe that a new semi-analytical model for late-time behavior can be obtained by means of the scaling equations presented in this paper.

NOMENCLATURE

- A = cross-sectional area
- CT = CT scanner number
- F = porosity
- H = height of the core
- k = permeability
- m = mass of water imbibed
- P = pressure
- S = saturation
- t = time
- t* = characteristic time
- x = horizontal distance
- y = vertical distance
- Y = vertical position of iso-saturation

- α = hydraulic diffusivity
- ρ = density
- μ = viscosity
- σ = interfacial tension

Subscripts.

a = air
aw = air and water saturated
c = capillary
cd = dry core
cw = 100% water saturated
D = dimensionless
f = fracture
i = injection
m = matrix
nw = non-wetting
o = out
w = water

ACKNOWLEDGMENT

This work was conducted with the financial support of the Stanford Geothermal Program under the US Department of Energy Grant No. DE-FG07-95ID13370, the Stanford University Petroleum Research Institute (SUPRI-A) Industrial Affiliates, and Consejo Nacional de Ciencia y Tecnología (CONACyT), México.

We thank Will Whitted for valuable help in the construction of the experimental set-up.

REFERENCES

Akin, S., Schembre, J.M., Bhat, S.K., and Kovscek, A.R.: "Spontaneous Imbibition Characteristics of Diatomite," submitted to Journal of Petroleum Science and Engineering, May 1999.

Carlsaw H.S., and Jaeger J.C.: "Conduction of Heat in Solids," Oxford Science Publications, Oxford University Press Inc., 1959.

Cil, M. and Reis, J.C.: "A Multi-Dimensional, Analytical Model for Counter -Current Water Imbibition into Gas-Saturated Matrix Blocks," J.Pet. Sci & Eng., **16**: 61-69, 1996.

Cil, M., Reis, J.C., Miller, M.A., and Misra, D.: "An Examination of Countercurrent Capillary Imbibition Recovery from Single Matrix Blocks and Recovery Predictions by Analytical Matrix/Fracture Transfer Functions," presented at the SPE Ann. Tech. Conf. And Exhibition, New Orleans, LA, 27-30 Sept., 1998.

Garg, A., Zwahlen, E., and Patzek, T.W.: "Experimental and Numerical Studies of One-Dimensional Imbibition in Berea Sandstone," presented at the 16th Annual American Geophysical Union Hydrology Days, Fort Collins, CO, 15-18 Apr, 1996.

Handy, L.: "Determination of Effective Capillary Pressure for Porous Media from Imbibition Data." Pet. Trans. AIME **219**: 75-80, 1960.

Hughes, R.G.: "CT Measurements of Two-Phase Flow in Fractured Porous Media," MS Report, Stanford University, Stanford, CA, 1995.

Kazemi, H., Gilman, J.R., and El-Sharkaway, A.M.: "Analytical and Numerical Solution of Oil Recovery from Fractured Reservoirs Using Empirical Transfer Functions." SPE19849, presented at the SPE 64th Ann. Tech. Conf. And Exhibition, San Antonio, TX, 8-11 Oct, 1989.

Ma, S., Morrow, N.R., and Zhang, X.: "Experimental Verification of a Modified Scaling Group for Spontaneous Imbibition." SPE30762, presented at the SPE Ann. Tech. Conf. And Exhibition, Dallas, TX 22-25 Oct., 1995.

Mattax, C., and Kyte, J.R.: "Imbibition Oil Recovery from Fractured Water-Drive Reservoirs." Soc. Pet. Eng. J. **2**: 177-184, 1962.

Mogensen, K., and Stenby, E.H.: "A Dynamic Two-Phase Model Pore-Scale Model of Imbibition," Transport in Porous Media, **32**: 299-327, 1998.

Morrow, N.R., Ma, S., Zhou, X., and Zhang, X.: "Characterization of Wettability from Spontaneous Imbibition Measurements." CIM 94-475, presented at the 45th Ann. Tech. Meeting of the Pet. Soc. Of the CIM, Calgary, Alberta Canada, 12-15 Jun., 1994.

Rangel-German, E.: " Experimental and Theoretical Investigation of Multiphase Flow in Fractured Porous Media," MS report, Stanford University, Stanford, CA, 1998.

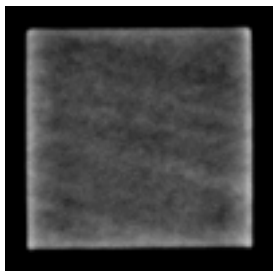
Rangel-German, E., Akin, S., and Castanier, L.: "Multiphase-Flow Properties of Fractured Porous Media," presented at the SPE Western Regional Meeting, Anchorage, AK, 26-28 May, 1999.

Reis, J.C. and Cil, M.: "A Model for Oil Expulsion by Counter-Current Water Imbibition in Rocks: One-Dimensional Geometry," J. Pet. Sci & Eng., **10**: 97-107, 1993.

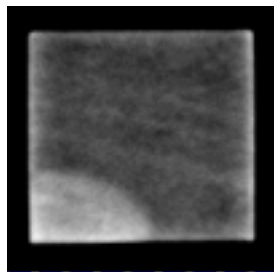
Reis, J. and Cil, M.: "Analytical Models for Capillary Imbibition: One-Dimensional Matrix Blocks." In Situ, **23(3)**, 243-270, 1999.

Reis, J.C. and Haq, S.A.: "Water Advance in a Single Fracture in the Presence of Capillary Imbibition into Adjacent Matrix Blocks." In Situ, **23(3)**, 271-295, 1999.

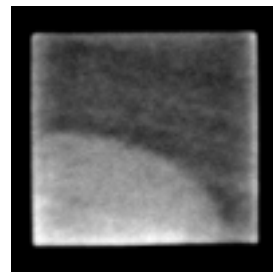
Zhang, X., Morrow, N.R., and Ma, S.: "Experimental Verification of a Modified Scaling Group for Spontaneous Imbibition." Soc. Pet. Eng. Res. Eng. **11**: 280-285, 1996.



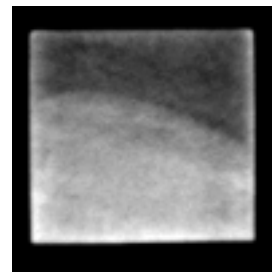
1 min (0.032PV)



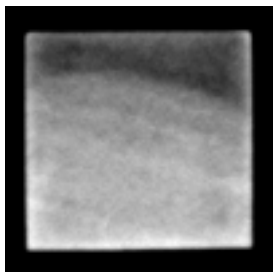
5 min (0.16 PV)



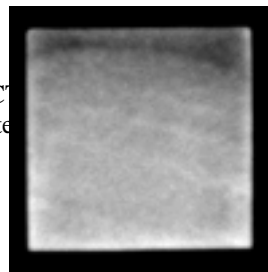
10 min (0.32 PV)



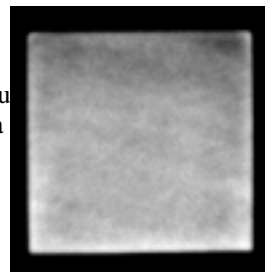
15 min (0.48 PV)



20 min (0.64 PV)



25 min (0.8 PV)



30 min (0.96 PV)

C
ate
ctu
a
mes.